Title no. 99-S8

Seismic Behavior of Concrete Columns Confined with Steel and Fiber-Reinforced Polymers

by Shamim A. Sheikh and Grace Yau

Results from an experimental program are presented in which 12 356 mm diameter and 1473 mm long columns were tested under constant axial load and reversed cyclic lateral load that simulated forces from an earthquake. Each specimen consisted of a column cast integrally with a 510 x 760 x 810 mm stub that represented a beam-column joint area or a footing. The test specimens were divided into three groups. The first group consisted of four columns that were conventionally reinforced with longitudinal and spiral steel reinforcement. The second group contained six reinforced concrete columns that were strengthened with carbon fiber-reinforced polymers (CFRP) or glass fiber-reinforced polymers (GFRP) before testing. The last group included two columns that were damaged to a certain extent, repaired with fiber-reinforced polymers (FRP) under axial load, and then tested to failure. The main variables investigated were axial load level, spacing of spirals, thickness, and type of FRP. From the results of the tests, it can be concluded that carbon and GFRP can be used effectively to strengthen deficient columns such that their behavior under simulated earthquake loads matches or exceeds the performance of columns designed according to the seismic provisions of the 1999 ACI Code. The use of FRP significantly enhances strength, ductility, and energy absorption capacity of columns.

Keywords: column; concrete; ductility; polymer; strength.

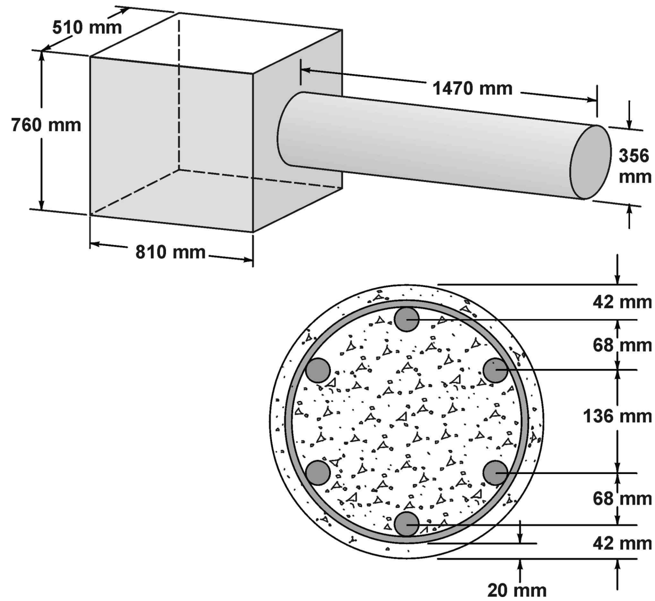

Fig. 1—Details of test specimen.

INTRODUCTION AND RESEARCH SIGNIFICANCE

Repair, rehabilitation, and strengthening of existing structures has become a major part of construction activity in North America. By some estimates, the money spent on retrofitting of existing structures in recent years has exceeded that spent on new structures. There are more than 200,000 bridges in North America that represent approximately 40% of the available inventory that are deemed deficient.[1] Some of these deficient bridges are damaged, while others need strengthening because either the design codes have changed, making these structures substandard, or larger loads are permitted on the road. A similar scenario of other components of infrastructure such as airports and parking garages. exists where extensive retrofitting is required. Procedures that are technically sound and economically feasible are needed to upgrade deficient structures. Traditional techniques that employ materials such as steel and cementitious composites have been used successfully for many applications, but have not proved very durable in many cases. For certain applications, the traditional techniques are very cumbersome and expensive. In the research presented herein,[2] relatively new materials, fiber-reinforced polymer (FRP), have been used to retrofit circular columns. Continuous fibers of carbon or glass were used in a circumferential direction to confine the columns. The main purpose of this study was to evaluate the effectiveness of FRP reinforcement in strengthening deficient columns or repairing damaged columns. This was achieved by comparing the behavior of FRP-retrofitted columns with that of conventionally reinforced columns. A standard lateral load sequence that simulated earthquake forces was used for all the columns. The same loading sequence was used for testing of over 60 similar steel reinforced concrete columns with square and rectangular cross sections.[3,4] A direct comparison can thus be made between the performance of all the columns.

EXPERIMENTAL PROGRAM

A total of 12 specimens were tested. Each specimen consisted of a 356 mm diameter and 1.47 m long column cast integrally with a 510 x 760 x 810 mm stub. All columns were tested under lateral cyclic loading while simultaneously being subjected to constant axial load throughout the test. The layout of the specimen is shown in Fig. 1. The column represented the part of a bridge column or a building column between the section of maximum moment and the point of contraflexure. The stub represented a discontinuity, such as a beam column joint or a footing. In all specimens, the ratio of the core area measured to the centerline of spiral to the gross area of the column section was kept constant at 74%, which is similar to that used in previous tests.[3-5]

ACI Structural Journal, V. 99, No. 1, January-February 2002.
MS No. 01-028 received February 8, 2001, and reviewed under Institute publication policies. Pertinent discussion will be published in the November-December 2002 *ACI Structural Journal* if received by July 1, 2002.

Shamim A. Sheikh, *FACI, is a professor of civil engineering at the University of Toronto, Ontario, Canada. He is Chair of ACI-ASCE Committee 441, Reinforced Concrete Columns, and is a member of ACI Committee 374, Performance-Based Seismic Design of Concrete Buildings. His research interests include earthquake resistance and seismic upgrade of concrete structures, confinement of concrete, use of FRP in concrete structures, and expansive cement and its applications. In 1999, he received the ACI Structural Research Award for a paper on the design of ductile concrete columns.*

Grace Yau *works as a structural engineer with Weiskopf and Pickworth, LLP, Consulting Engineers in New York City. She received her Masters of Applied Science in 1998 from the University of Toronto.*

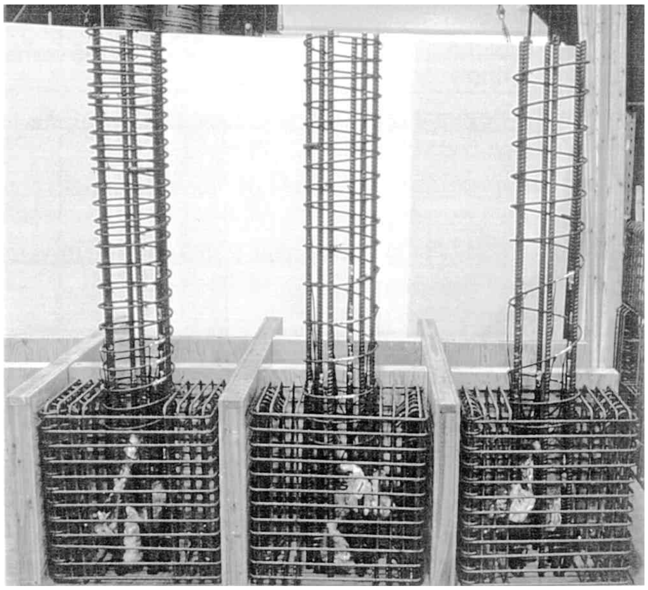

Fig. 2—Reinforcing cages of specimens.

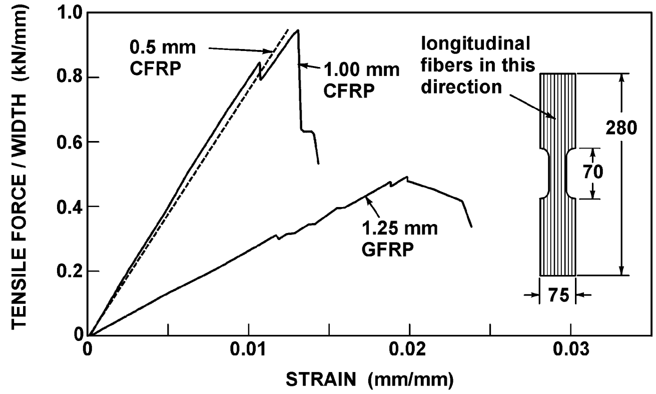

Fig. 3—Tensile force-strain curves for FRP composites.

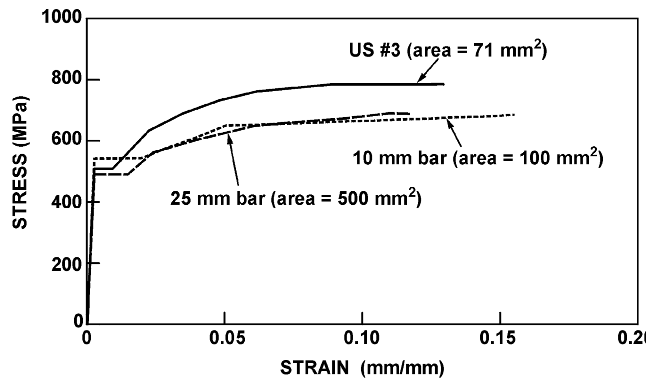

Fig. 4—Tensile stress-strain curves for reinforcing steel bars.

Table 1 gives the details of the test specimens. All the columns contained six 25M (500 mm^2) longitudinal steel bars, and the spirals were made of U.S. No. 3 (71 mm^2) bars. The reinforcement for the stub consisted of 10M (100 mm^2) horizontal and vertical stirrups at 64 mm spacing. In addition, 10M bars with 135 degree hooks were placed at the top and bottom of the stub at the same spacing (Fig. 2). The longitudinal bars in the columns were completely extended into the stub, whereas the spiral reinforcement was extended into the stub for 100 mm. The design of the specimens aimed at forcing the failure in the potential plastic hinge region of the column, that is, within a length of 800 mm from the face of the stub. The length of 800 mm was chosen based on previous tests[3,4] where it was observed that the length of the most damaged region of the column was approximately equal to the section depth and located approximately 100 to 200 mm away from the stub. Outside the test region, the spacing of spiral reinforcement was reduced to around 2/3 of the specified spacing in the test zone (Fig. 2). All specimens were cast together in vertical positions.

The test specimens are divided into three groups. The first group, Series S, consisted of columns S-1NT, S-2NT, S-3NT, and S-4NT. Only steel spirals were used as lateral reinforcement in these columns. Specimens S-1NT and S-2NT contained the amount of spiral reinforcement that satisfied the 1999 ACI Code[6] provisions for seismic resistance, whereas Specimens S-3NT and S-4NT contained much less spiral reinforcement (Table 1). These four columns were tested to failure to establish the standard behavior against which columns retrofitted with FRP could be compared. The second group, Series ST, consisted of six columns that contained the same amount of spiral reinforcement as Specimens S-3NT and S-4NT; however, they were strengthened with GFRP or CFRP before testing. Specimens ST-1NT to ST-6NT fall in this group. The third group, Series R, included Specimens R-1NT and R-2NT that contained 50% less spiral reinforcement compared with Specimens S-1NT and S-2NT. These two columns were damaged to a certain extent under axial and lateral loads, repaired under axial load with FRP, and then tested to failure.

For Specimens ST-1NT and ST-2NT, the FRP composite was wrapped within the potential plastic hinge zones of the columns, that is, for a length of approximately 800 mm starting from the stub face, and the failure occurred in the test zone. During the testing of Specimen ST-3NT, however, crushing of concrete was observed outside the test region; therefore, to ensure that the failure took place within the plastic hinge zone, it was decided to wrap the whole column for the rest of the specimens. Column ST-6NT was strengthened with four 100 mm wide CFRP bands at a clear spacing of 100 mm. The first band was applied at a distance of 50 mm from the stub face. The glass fabric was 1.25 mm thick, whereas the carbon fabric was either 0.5 or 1.0 mm thick. The type of fabric and the number of layers used were designed to study a range of parameters for their effects on column behavior.

Fiber-reinforced polymer (FRP)

A commercially available FRP system was used for retrofitting. The epoxy consisted of two components, A and B, which were mixed for 5 min with a mixer at a speed of 400 to 600 rpm. The mixing ratio was 100 parts of A to 42 parts of B by volume. The carbon or glass fabric was saturated

Table 1—Details of test specimens

Specimen	Lateral reinforcement in test zone: Size	Spacing, mm	ρ_s	Treatment	Axial load ratio P/P_o	f_c', MPa	Energy damage indicator E
Group I: Series S							
S-1NT	US No. 3	80	1.12	Control	0.54	40.1	69
S-2NT	US No. 3	80	1.12	Control	0.27	40.1	778
S-3NT	US No. 3	300	0.30	Control	0.54	39.2	5
S-4NT	US No. 3	300	0.30	Control	0.27	39.2	9
Group II: Series ST							
ST-1NT	US No. 3	300	0.30	Strengthened with 1 layer of 1.25 mm GFRP	0.54	40.4	—
ST-2NT	US No. 3	300	0.30	Strengthened with 1 layer of 1.25 mm GFRP	0.54	40.4	181
ST-3NT	US No. 3	300	0.30	Strengthened with 1 layer of 1.00 mm CFRP	0.54	40.4	202
ST-4NT	US No. 3	300	0.30	Strengthened with 1 layer of 0.50 mm CFRP	0.27	44.8	1028
ST-5NT	US No. 3	300	0.30	Strengthened with 1 layer of 1.25 mm GFRP	0.27	40.8	1040
ST-6NT	US No. 3	300	0.30	Strengthened with 1.00 mm CFRP bands	0.27	41.6	78
Group III: Series R							
R-1NT	US No. 3	160	0.56	Damaged and repaired with 2 layers of 1.25 mm GFRP	0.54	42.8	192* 310†
R-2NT	US No. 3	160	0.56	Damaged and repaired with 1 layer of 1.00 mm CFRP	0.54	43.9	31* 86†

*Based on ϕ_1 of repaired specimen.
†Based on ϕ_1 of original specimen.

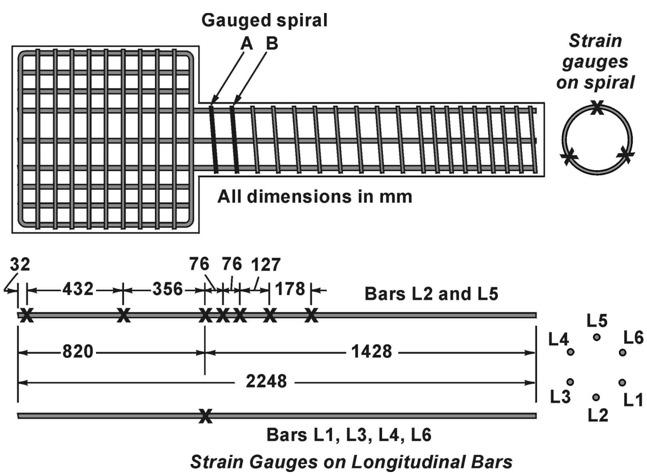

Fig. 5—Location of strain gages on longitudinal and spiral reinforcement.

with the epoxy, and a layer of epoxy was also applied to the surface of the column. The saturated fabric was then wrapped around the column with fiber orientation in the circumferential direction, with an overlap length of 100 mm. The thickness of epoxy was not strictly controlled, and excess amounts were squeezed out along with any air bubbles.

Three types of fabrics were used in this test series. The test coupons were made from the fabric impregnated with epoxy and cured to harden. Figure 3 shows details of a typical test specimen and the tensile stress-strain curves for the three types of FRP. Each curve is the average of at least three tests. Since the thickness of the composite depends on the amount of epoxy used, the tensile strength is represented in force per unit width instead of stress.

Concrete

Ready mixed concrete with a specified compressive strength of 30 MPa was used. Development of concrete strength with age was monitored by testing two or three cylinders at one time. The strength of unconfined concrete in a particular specimen was obtained from the strength-age curve for the age of that specimen and varied between 39 and 45 MPa.

Steel

Deformed bars were used in all the specimens. Grade 400, 25M bars were used to provide longitudinal steel contents of 3.0% in all the columns. U.S. No. 3, Grade 60 steel was used for spiral reinforcement. Reinforcement in the stub was provided by a Grade 400, 10M bar. Figure 4 shows the stress-strain curves for the three types of steel. Each curve shown represents an average of at least three test results.

Patching materials

Two types of patching materials were used for column repair. High-early-strength mortar was prepared by mixing fine sand with Type I portland cement in equal amounts by weight. The water-cement ratio was 0.15. The compressive strength of the mortar reached 40 MPa in 2 days. The second material was a commercially available shrinkage-compensated mortar called EMACO S77-CR. It can be mixed with water at a ratio of 14 to 18.5% by weight and yields a compressive strength of 25 to 57 MPa in 7 days.

Instrumentation

Each specimen had a total of 18 strain gages installed on the longitudinal reinforcement. Moreover, the spiral reinforcement within the test region was instrumented with three strain gages on each turn. Specimens S-1NT and S-2NT had nine strain gages each attached to the spiral reinforcement, and all other specimens had six. Figure 5 shows the locations of the strain gages. The concrete core deformations were measured using 18 linear variable displacement transducers (LVDTs) with 10 on one side and 8 on the other side. The gage lengths varied from 75 to 120 mm and covered a length of about 515 mm. Transverse displacements of each specimen were also measured at six different locations along its length using LVDTs.

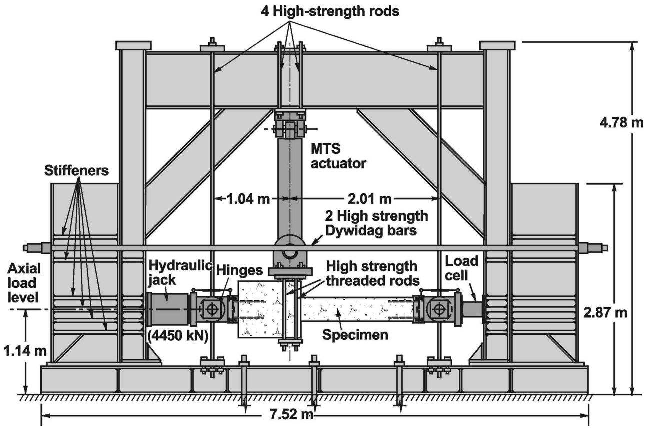

Fig. 6—Test setup.

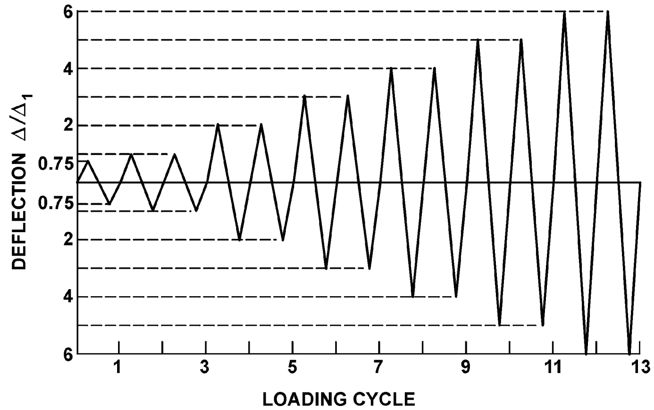

Fig. 7—Specified displacement history.

Fig. 8—Damaged regions of Specimen R-2NT.

Testing

The test setup is shown in Fig. 6. A hydraulic jack with a capacity of 4450 kN was used to apply the axial load that was measured by a load cell. The cyclic lateral load was applied by an actuator with a 1000 kN load capacity and a ±150 mm stroke capacity. A displacement control mode of loading was used in all the tests to apply a predetermined displacement history. The testing apparatus was specially designed to allow in-plane rotation of test specimens. Prior to testing, each specimen was aligned both vertically and horizontally until the centerline of the specimen matched the line of action of axial load. All specimens were subjected to inelastic cyclic loading while simultaneously carrying a constant axial load throughout the test. The lateral load sequence (Fig. 7) consisted of one cycle to a displacement of $0.75\Delta_1$ followed by two cycles each to Δ_1, $2\Delta_1$, $3\Delta_1$ ... and so on, until the specimen was unable to maintain the applied axial load. Deflection Δ_1 was defined as the lateral deflection corresponding to the maximum lateral load along a line that represented the initial stiffness of the specimen. The lateral deflection Δ_1 was calculated using the theoretical sectional behavior of the column and integrating curvatures along the length of the specimen. This loading sequence is similar to the one used previously by Sheikh and Khoury.[3]

TEST OBSERVATIONS

The first signs of distress in all test specimens were the cracks in the cover concrete at the top and the bottom (Fig. 6). For the S series specimens (Group I), it was at the first peak of the fourth cycle, that is, $\Delta = 2\Delta_1$, that the cover at the top spalled followed by spalling of the cover at the bottom at the second peak. In all the S series specimens (Group I), the most extensive damage was concentrated approximately 295 to 350 mm from the stub face. Spalling of the cover, however, extended from close to the stub for a distance of about 585 to 740 mm. During the last cycle, buckling of the longitudinal bars was observed after yielding of the spiral reinforcement, which indicated the commencement of failure. In Specimens S-3NT and S-4NT, however, the spiral reinforcement did not yield. Fracture of the spiral occurred in Specimens S-1NT and S-2NT and brought about the termination of the tests. For the ST series specimens, separation of the FRP fabric from concrete along the circumference was observed within the hinging zone, as indicated by a change in FRP color, during the fourth or fifth cycle when the concrete crushed. As the applied displacement increased, this separation in the FRP wraps extended for a distance of 200 to 400 mm from close to the stub. During testing of Specimen ST-3NT, crushing of concrete outside the test region was observed in the ninth cycle ($\Delta = 4\Delta_1$). The test was stopped immediately by bringing the specimen to zero displacement, and the axial load was reduced to half of its original level. The column outside the test region was then strengthened with two layers of CFRP. After that, the test was continued by increasing the axial load to the original. In most cases, during the last loading cycle, rupture of FRP at the bottom of the columns occurred along with the buckling of longitudinal reinforcing bars, which was an indication that failure had begun.

Specimen ST-1NT failed in an unpredictable manner. The GFRP composite split along the extruded reinforcing bars used for LVDT mounts at a distance of 390 to 560 mm from the stub face. It is believed that during wrapping of the column, the GFRP was weakened by the extruded LVDT bars, which in turn caused premature rupture of the composite. To avoid this type of failure, one additional FRP strip with a width of 75 mm was installed along the extruded LVDT bars on all other specimens. In the case of Specimen ST-6NT, failure was initiated by debonding of the CFRP bands. During the eighth cycle ($\Delta = 4\Delta_1$), the first CFRP band adjacent to the stub debonded followed by the second one in the next cycle, which brought about the termination of the test. The most extensive damage for all of the columns with FRP wraps concentrated at approximately 250 to 300 mm from the stub face, which is also the location of the first fiber rupture. The failure mode for all specimens was dominated by flexural effects. No cracking was seen in the stub in any specimen.

Specimen R-1NT was subjected to three load cycles, that is, maximum displacement of Δ_1 when cracks formed at both top and bottom. The specimen was further damaged with two cycles of $1.4\Delta_1$. Vertical flexural cracks were observed in the hinging zone at a distance of approximately 100 to 400 mm from the stub face. Some spalling of top cover occurred at a

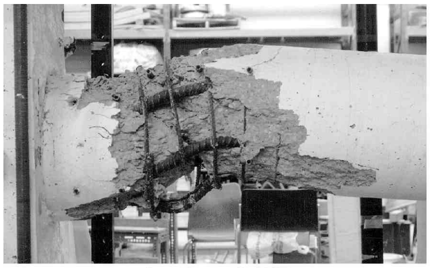

Specimen S-1NT

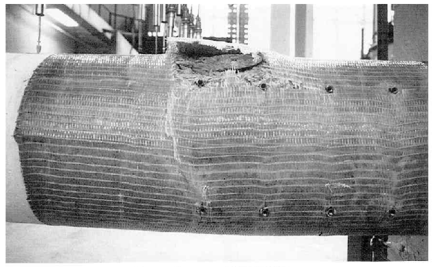

Specimen ST-1NT

Specimen ST-5NT

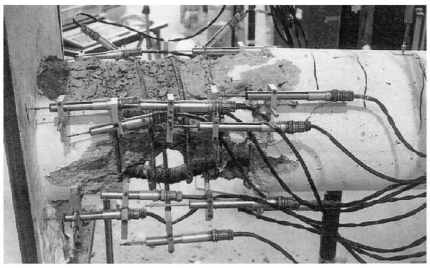

Specimen S-2NT

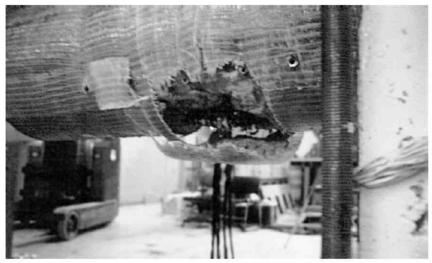

Specimen ST-2NT

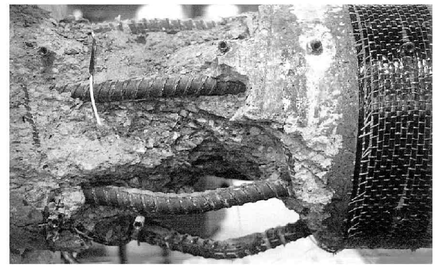

Specimen ST-6NT

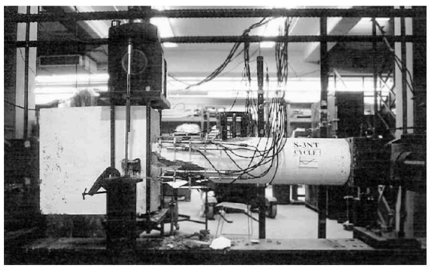

Specimen S-3NT

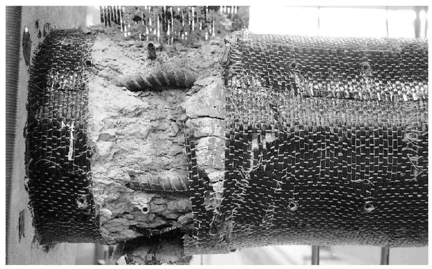

Specimen ST-3NT

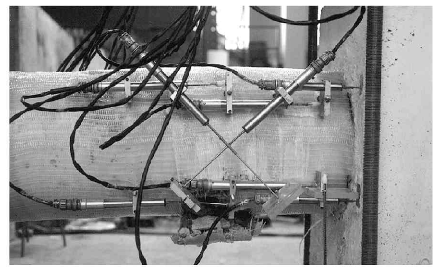

Specimen R-1NT

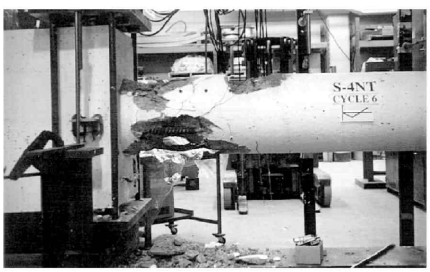

Specimen S-4NT

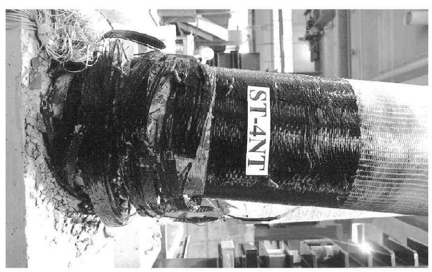

Specimen ST-4NT

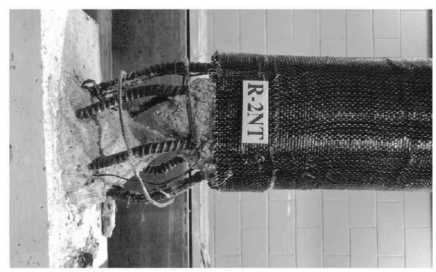

Specimen R-2NT

Fig. 9—Specimens after testing.

distance of 435 to 685 mm from the stub. Yielding of longitudinal reinforcement was also observed. Inadvertently, Specimen R-2NT was damaged more extensively. It was loaded up to the fifth cycle, that is, maximum displacement of $2\Delta_1$, which resulted in the yielding of both longitudinal and spiral reinforcement. The top cover spalled off between 150 and 550 mm from the stub, while the bottom cover was lost for a distance of approximately 500 mm from close to the stub (Fig. 8).

The damaged columns were repaired while they were subjected to 2/3 of the originally applied axial load. The loose concrete was first removed in both columns. A high-early-strength mortar was used for patching Column R-1NT, while for Column R-2NT, the structural repair mortar EMACO S77-CR was used. The repair mortar was cured for 2 days before the FRP was wrapped around the columns as detailed in Table 1. Observations made during the testing of the two repaired columns were similar to those of specimens in the ST series (Group II), except that in the case of Specimen R-2NT, rupture of the fibers was caused by the fracture of the spiral reinforcement during the last loading cycle. Figure 9 shows the specimens at the end of the tests.

RESULTS AND DISCUSSION

Figure 10 shows the idealization of a test specimen. Response of each specimen can be obtained in the form of applied lateral load-displacement at column-stub connection P_L-δ, shear force-tip deflection V-Δ, and moment-curvature M-ϕ curves following the procedure used for previous specimens.[3] The curvature was computed using the deformation readings measured by upper and lower LVDTs located at the most damaged region within the hinging zone. The moment shown was also calculated at the same location. The moment M consists of two parts: the primary moment caused by the lateral load, and the secondary moment caused by the axial load. It should be noted that although the column section adjacent to the stub was subjected to the maximum moment, failure in all the columns initiated at a location that was approximately 200 to 400 mm away from the stub. The additional confinement provided by the stub strengthened

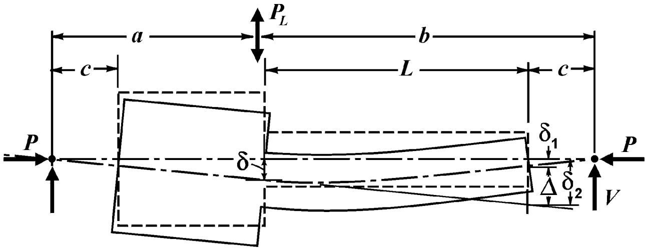

Fig. 10—Idealization of test specimen.

the critical section such that the failure took place at a lesser moment away from the stub. The V-Δ and M-ϕ responses of Specimen S-1NT are shown in Fig. 11. For the rest of the specimens, only the moment-curvature curves are presented herein (Fig. 12). Important events during testing such as spalling of the concrete cover, yielding of the spiral, buckling of the longitudinal bars, fracture of the spiral, and rupture of the FRP are marked on the graphs.

There were reasonable similarities in form between the V-Δ and M-ϕ plots for all the specimens. Of primary concern herein is the section behavior in the plastic hinge zone, as represented by the M-ϕ relationship because in the postelastic region further lateral displacement will take place as a result of plastic rotation at the critical section of the column. A number of variables can be examined by comparing different specimens. Among the steel reinforced specimens (Group I), effects of the level of axial load and the amount of spiral reinforcement and spiral pitch can be examined. In Group II specimens, the type of fiber used in FRP, amount of FRP reinforcement, and the level of axial load are the main variables that can be studied. Specimens in Groups II and III can be compared with those in Group I to evaluate the beneficial effects of using FRP and the effect of pre-existing damage before the columns are repaired.

Ductility parameters

Ductility in elastoplastic structures can be defined easily. In reinforced concrete members lacking such characteristics, however, there is no universal definition for ductility. Figure 13 describes various ductility parameters that have been used for steel reinforced concrete members.[3,4] These include curvature ductility factor μ_ϕ, cumulative ductility ratio N_ϕ and energy damage indicator E. All of the terms are defined in Fig. 13 except L_f and h, which represent the length of the most damaged region measured from the test and the depth of the column section, respectively. In members where no strength degradation takes place and the section capacity keeps increasing with increased deformation until failure, toughness and energy dissipation characteristics may define the section performance better than other ductility parameters. Table 1 lists the total energy damage indicator for all the columns.

Axial load level

Axial load level in a column is generally indicated by two indexes, $P/f_c'A_g$ and P/P_o, where A_g = gross cross-sectional area of the column. Sheikh, Shah, and Khoury,[4] based on an analysis of columns with f_c' ranging from approximately 30 to 60 MPa, concluded that for different f_c' values, a comparison of the behavior of columns using the index $P/f_c'A_g$ does not remain valid. They recommended the use of index P/P_o to evaluate the relative performance of columns, particularly with regard to ductility.

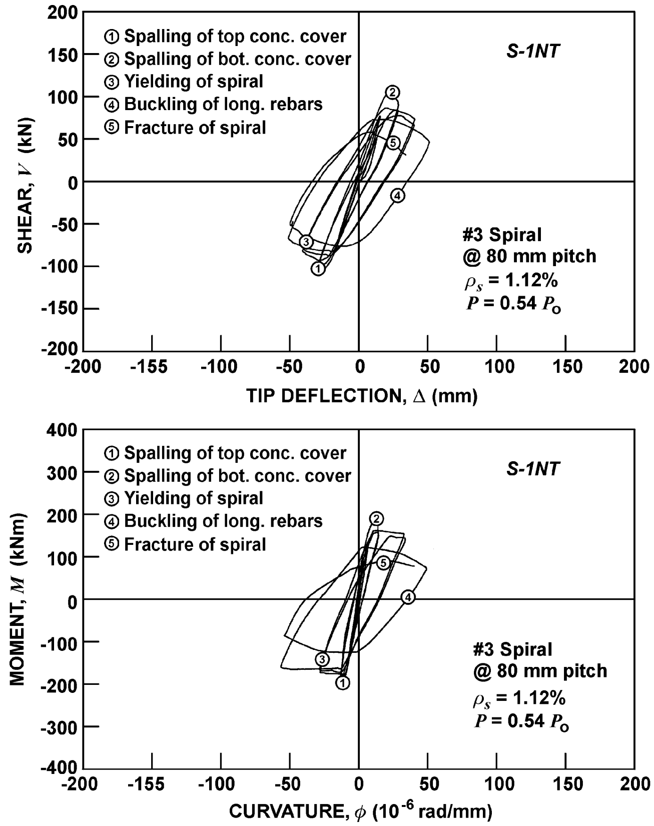

Fig. 11—Behavior of Specimen S-1NT.

Responses of Specimens S-1NT and S-2NT can be compared to evaluate the effects of axial load level. Specimen S-1NT was tested under an axial load of $0.54P_o$ while in S-2NT, the axial load was $0.27P_o$. Both specimens were identical in all other aspects. It is evident that an increase in axial load resulted in reduced ductility and deformability of the column. The energy dissipation capacity of the section under lower axial load is more than 10 times that of the section under high axial load. Another pair of steel reinforced specimens, S-3NT ($P = 0.54P_o$) and S-4NT ($P = 0.27P_o$) can also be studied for the effect of axial load. The amount of spiral reinforcement in both of these columns is only approximately 30% of that required by the ACI code.[6] Column behavior even under lower axial load was quite brittle, but the column was able to undergo five cycles of lateral load excursions and failed in the sixth cycle after undergoing a displacement of $3\Delta_1$. The Specimen S-3NT with $P = 0.54P_o$ failed in the fifth cycle with a maximum displacement of $2\Delta_1$. The only variable different between FRP-retrofitted Specimens ST-1NT and ST-5NT is the axial load level. Since Specimen ST-1NT failed prematurely, a direct comparison of the two specimens cannot be made. The results, however, clearly indicate the adverse effects of high axial load on the column's ductility.

Amount and spacing of spiral reinforcement

The effect of the amount and spacing of spiral reinforcement can be examined by comparing the behavior of Specimen S-1NT with that of S-3NT and the behavior of S-2NT with that of S-4NT. An increase in the amount of transverse reinforcement provides higher confining pressure, and the reduced spiral pitch improves the stability of the longitudinal bars, thus resulting in better ductile behavior of the columns. The energy dissipation capacities of the columns with more spiral rein-

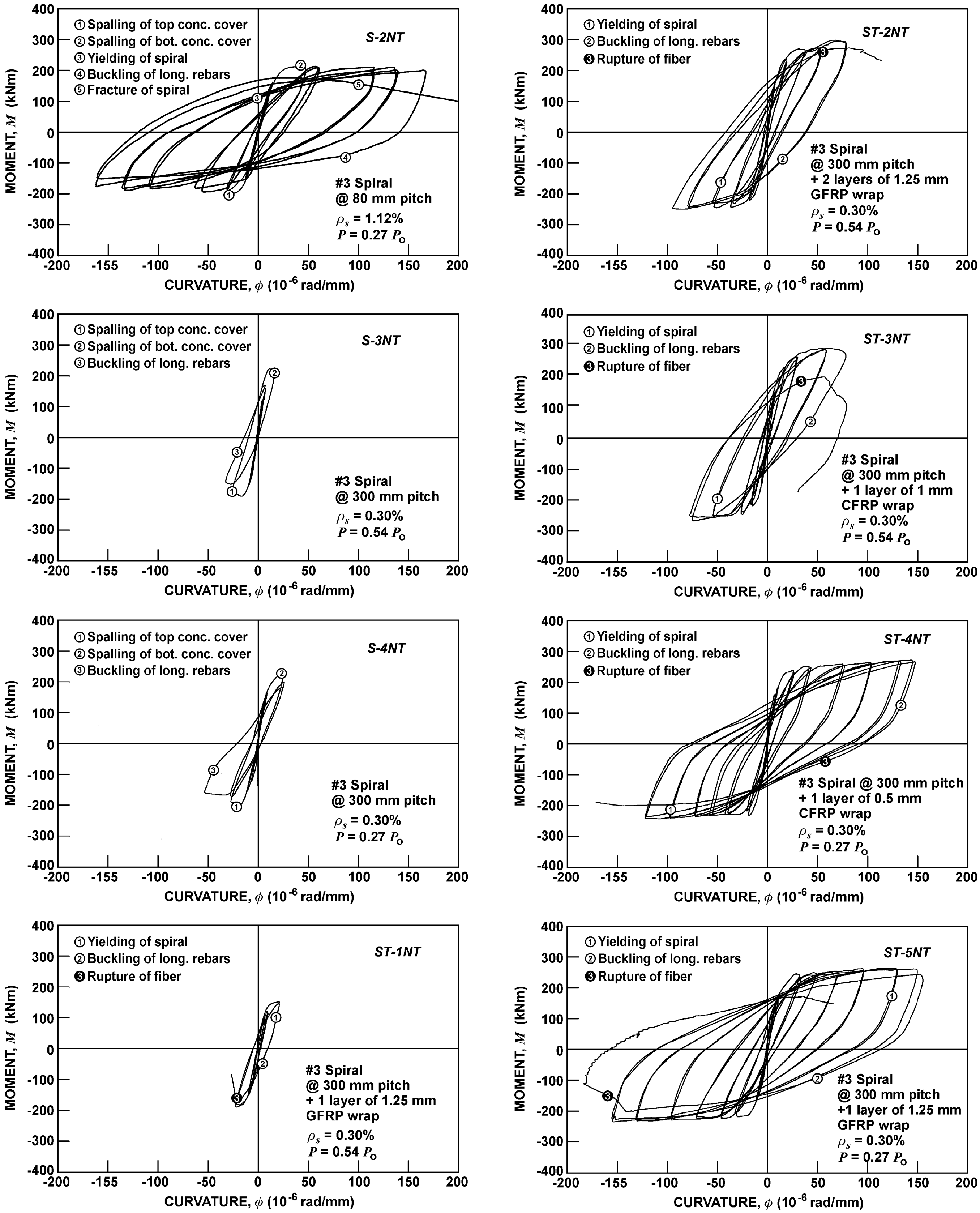

Fig. 12—Moment versus curvature responses.

forcement are orders of magnitude larger than that of specimens with smaller amounts of spiral steel.

Retrofitting with FRP

The effectiveness of strengthening deficient columns with FRP is evaluated by considering two sets of specimens. The first set was tested under an axial load of $0.54P_o$, while the axial load for the second set was $0.27P_o$. The first set includes Specimens S-1NT, S-3NT, ST-1NT, ST-2NT, and ST-3NT (Table 1; Fig. 11 and 12). Specimen S-3NT was similar to Specimens ST-1NT, ST-2NT, and ST-3NT in all respects except for the lack of FRP. Both Specimens S-3NT

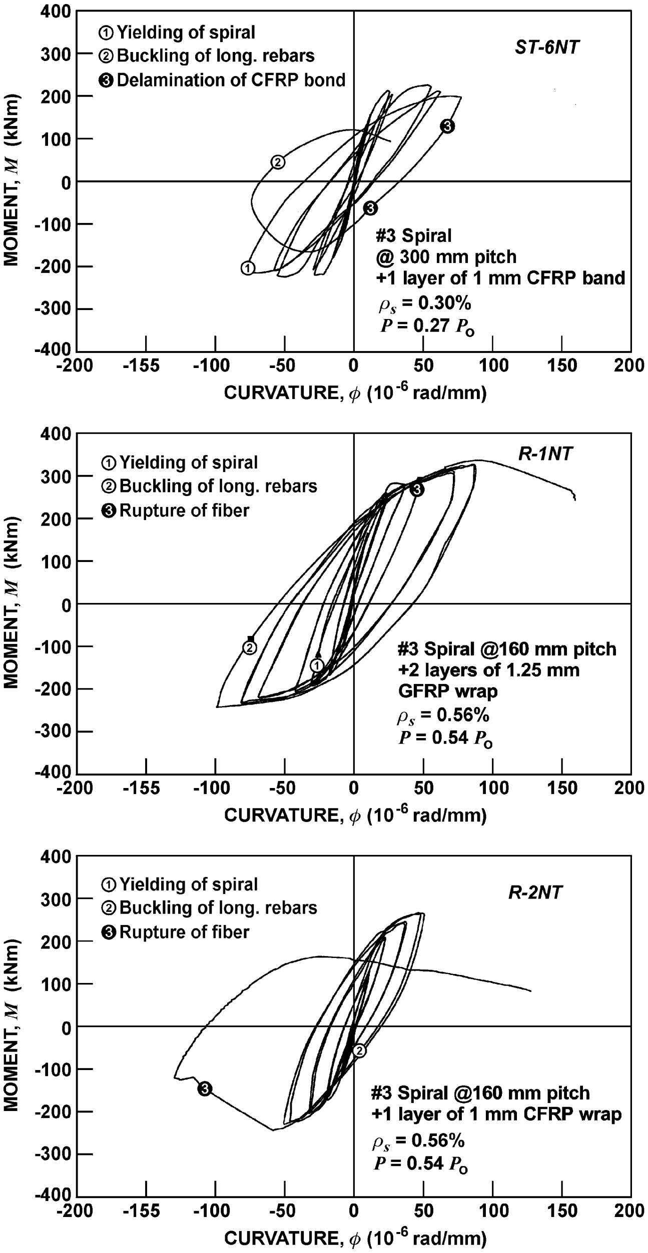

Fig. 12 (cont.)—Moment versus curvature responses.

and ST-1NT behaved in a very brittle manner, and the energy dissipation capacity in each specimen was poor. As mentioned previously, failure of Specimen ST-1NT was caused by premature rupture of the GFRP composite along the extruded LVDT bars. No improvement was therefore observed due to the strengthening by one layer of GFRP wrap in Specimen ST-1NT. Comparisons of the behavior of Specimen S-3NT with those of ST-2NT and ST-3NT show the remarkable beneficial effects of FRP wrapping on strength and ductility of columns. While Specimen S-3NT failed during the fifth load cycle (maximum displacement of $3\Delta_1$), Specimens ST-2NT and ST-3NT, retrofitted with two layers of GFRP and one layer of CFRP, respectively, were able to sustain 12 load cycles with a maximum displacement of $6\Delta_1$ and 11 load cycles with a maximum displacement of $5\Delta_1$, respectively. The energy dissipation capacity of the critical sections of the columns increased by a factor of approximately 40 due to retrofitting with glass and CFRP. The adverse effect of the reduced amount of spiral reinforcement

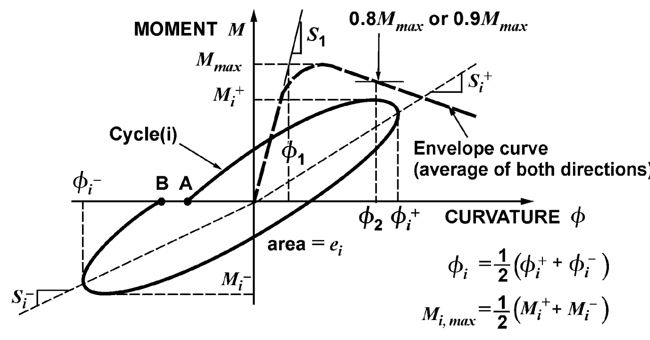

$$\phi_i = \frac{1}{2}(\phi_i^+ + \phi_i^-)$$

$$M_{i,max} = \frac{1}{2}(M_i^+ + M_i^-)$$

$$S_i = \frac{1}{2}(S_i^+ + S_i^-)$$

$$\mu_\phi = \frac{\phi_2}{\phi_1} \qquad N_\phi = \sum_{i=1}^{i=m} \frac{\phi_i}{\phi_1} \qquad E = \frac{1}{M_{max}\phi_1} \sum_{i=1}^{i=m} e_i \frac{L_f}{h} \left(\frac{S_i}{S_1}\right) \left(\frac{\phi_i}{\phi_1}\right)^2$$

Fig. 13—Definitions of ductility parameters.

and larger spiral spacing in S-3NT compared with S-1NT is more than compensated by the additional confinement provided by the FRP wraps. It should be noted that Specimens ST-2NT and ST-3NT had no strength degradation; the section moment capacity kept increasing until failure. Behavior of the two FRP-strengthened specimens was even better than that of Specimen S-1NT in which the spiral reinforcement satisfied the seismic code provisions of the ACI code.[6] A comparison of Specimens ST-2NT and ST-3NT shows that two layers of GFRP results in the improvement of column behavior similar to that obtained using one layer of CFRP.

The second set of columns that were tested under $P = 0.27P_o$ includes Specimens S-2NT, S-4NT, ST-4NT, ST-5NT, and ST-6NT (Table 1 and Fig. 12). Specimen S-4NT was identical to Specimens ST-4NT, ST-5NT, and ST-6NT in all respects except for the lack of FRP. Similar to the first set, specimens strengthened with FRP displayed higher energy dissipation capacity and strength than Specimen S-4NT. The seismic resistance of retrofitted columns improved significantly as a result of the confining action of the FRP composite wraps. The overall responses of Specimens ST-4NT and ST-5NT, retrofitted with one layer of GFRP and one layer of 0.5 mm thick CFRP, respectively, were similar to or better than those of Specimen S-2NT in which the spiral reinforcement was designed according to the seismic code provisions of the ACI code.[6] The FRP-retrofitted Specimens ST-4NT and ST-5NT did not show a significant descending part in their responses until the end of the test unlike Specimen S-2NT, which showed some strength loss with increased displacement excursions. Specimens ST-4NT and ST-5NT displayed very similar responses, which indicated that the column retrofitted with one layer of 0.50 mm CFRP performs as well as that with one layer of 1.25 mm GFRP. A thinner (0.5 mm) carbon fabric was selected for Specimen ST-4NT taking into consideration that it will provide half as much confining pressure as expected from a 1.0 mm carbon fabric in Specimen ST-3NT. It was later found, however, that the strength of 0.5 mm thick CFRP in N/mm width was similar to that of 1.0 mm thick CFRP, which indicates a better quality fiber for thinner fabric (Fig. 3). Under an axial load of $0.27P_o$, which is approximately equal to a balanced load, one layer of FRP increased the energy dissipation capacity of the section by a factor of more than 100.

The behavior of Specimen ST-6NT retrofitted with bands of CFRP was more ductile and stable than Specimen S-4NT, but not as good as S-2NT. As mentioned previously, failure of Specimen ST-6NT was induced by debonding of the first two CFRP bands adjacent to the column-stub interface. As the first CFRP band debonded, the column started to deteriorate due to the loss of confinement. When debonding of the second band occurred, the column was unable to maintain the axial load and failed rapidly. The lap splice used for the FRP was approximately 105 mm.

From a comparison of Specimens ST-3NT and ST-4NT, it can be seen that the amount of confinement required to produce comparably ductile behavior depends on the level of axial load. Specimen ST-4NT, tested under an axial load of $0.27P_o$, displayed considerably more ductile behavior than Specimen ST-3NT in which the axial load was $0.54P_o$. Both columns were confined to a similar degree with equivalent lateral CFRP reinforcement. A similar conclusion can also be drawn by comparing Specimens ST-2NT and ST-5NT. It appears that a two-fold increase in the axial load requires more than twice the amount of lateral reinforcement for a comparable improvement in a column's ductile performance.

The original Specimens R-1NT and R-2NT were identical in all respects and were tested under an axial load of $0.54P_o$. They were damaged to a certain extent, repaired with FRP while subjected to axial loads, and then tested to failure. Specimen R-1NT was repaired with two layers of GFRP, while Specimen R-2NT was wrapped with one layer of CFRP. The repaired specimens were tested under the same high axial load level until failure. The behavior of Specimen R-1NT was more ductile than that of Specimen R-2NT, and its sectional response was also relatively stiffer. This appears to be partly due to the fact that Specimen R-2NT was more extensively damaged than R-1NT as mentioned previously. It should be noted, however, that the lateral load and section capacity of both repaired columns kept increasing with every load cycle until failure. The responses of Specimens R-1NT and R-2NT exceeded the performance of Specimen S-1NT that was designed according to the seismic provisions of the ACI code.[6] Repaired Specimens R-1NT and R-2NT were comparable in performance, respectively, to Specimens ST-2NT and ST-3NT that were strengthened without damage. From the test results, it can be concluded that the amount of confinement required for repair depends on the extent of damage inflicted on the member.

SUMMARY AND CONCLUSIONS

Results from an experimental program are presented in which 12 column specimens were tested under constant axial load and cyclic lateral load excursions that simulated earthquake forces. Each specimen consisted of a 356 mm diameter and 1.47 m long column cast integrally with a 510 x 760 x 810 mm stub that represented a beam-column joint area or a footing. Four columns were reinforced conventionally with longitudinal and spiral steel. Of the remaining eight columns, six were strengthened with carbon or GFRP before testing, and two columns were tested to a certain damage level, repaired with FRP under axial load, and retested to failure. FRP was used only in the transverse direction of the column section to confine concrete. The following conclusions can be drawn from this study.

1. Use of carbon and GFRP resulted in remarkable improvement in the performance of columns, resulting in large increases in ductility, energy dissipation capacity, and strength. For a column subjected to an axial load equal to $0.27P_o$, which is approximately equal to a balanced load, one layer of carbon or GFRP increased the energy dissipation capacity by a factor of more than 100;

2. Unlike the internal spiral reinforcement that only confines the core concrete, the FRP wraps effectively confine the entire column section. The behavior of FRP retrofitted columns under simulated earthquake loads matched or exceeded the performance of slab-reinforced columns designed according to the seismic provisions of the ACI Code;[6]

3. In steel reinforced columns, section and member ductility decreased significantly with an increased spiral pitch and reduced amount of spiral reinforcement. The adverse effects of a reduced amount of spiral reinforcement and larger spacing can be compensated for by the confinement provided by FRP;

4. Column ductility deteriorates as the level of axial load increases. The amount of FRP reinforcement needed to improve column behavior depends on the level of axial load. It was observed that the amount of FRP reinforcement required under an axial load of $0.54P_o$ is slightly more than twice that needed for an axial load of $0.27P_o$ for similar performance enhancement;

5. Columns retrofitted with FRP showed little strength degradation with increased displacement excursions until failure; and

6. FRP composites are very effective for the rehabilitation of damaged columns. The amount of FRP needed and the performance achieved is influenced by the extent of damage.

ACKNOWLEDGMENTS

The research reported herein was supported by a Strategic Grant from Natural Sciences and Engineering Research Council (NSERC) of Canada and a grant from Intelligent Sensing for Innovative Structures (ISIS), an NSERC Network of Centers of Excellence. Financial and technical support from Fyfe and Co., R. J. Watson, Inc., Roadsavers International, and Petro-Canada is gratefully acknowledged. The experimental work was carried out at the Structures Laboratories in the Department of Civil Engineering at the University of Toronto. Assistance from the technical staff is greatly appreciated.

NOTATION

A_c = area of concrete in column cross section
A_g = gross cross-sectional area of column
A_s = area of longitudinal steel in column
E = energy damage indicator
f_c' = compressive strength of concrete as measured from standard (150 x 300 mm) cylinder
f_y = yield strength of longitudinal steel
h = depth of column section
L_f = length of most damaged region of column
M = bending moment
N_ϕ = commutative ductility ratio
P = axial load on column
P_L = applied lateral load
P_o = axial load capacity of column = $0.85f_c' (A_g - A_c) + A_s f_y$
V = shear stress
Δ = tip deflection in column
δ = deflection in column
ϕ = curvature of section
μ_ϕ = curvature ductility factor

REFERENCES

1. Dunker, K. F., and Rabbat, B. G., "Why America's Bridges are Crumbling," *Scientific American*, Mar. 1993, pp. 66-72.

2. Yau, G., and Sheikh, S. A., "Repair and Strengthening of Columns with Fiber Reinforced Composites," *Research Report*, Department of Civil Engineering, University of Toronto, Toronto, Canada, Jan. 1998, 144 pp.

3. Sheikh, S. A., and Khoury, S. K., "Confined Concrete Columns with Stubs," *ACI Structural Journal*, V. 90, No. 4, July-Aug. 1993, pp. 414-431.

4. Sheikh, S. A.; Shah, D. V.; and Khoury, S. S., "Confinement of High-Strength Concrete Columns," *ACI Structural Journal*, V. 91, No. 1, Jan.-Feb. 1994, pp. 100-110.

5. Sheikh, S. A., and Uzumeri, S. M., "Strength and Ductility of Tied Concrete Columns," *Journal of the Structural Division*, ASCE, V. 6, No. ST5, May 1980, pp. 1079-1102.

6. ACI Committee 318, "Building Code Requirements for Structural Concrete (ACI 318-99) and Commentary (318R-99)," American Concrete Institute, Farmington Hills, Mich., 1999, 391 pp.